Asian Journal of Chemical and Environmental Research, Vol. 4 (3-4), 18-22, July - October (2011)

AJCER
Asian Journal of Chemical and Environmental Research

STUDY OF ATMOSPHERIC WAVES OVER LOW LATITUDE STATION KOLHAPUR USING NIGHT AIRGLOW TECHNIQUE

R. N. GHODPAGE*[1], P.T. PATIL[1], S.S. NIKTE[2], M.V.ROKADE[2] U. S. JAGTAP[3] AND A. K. SHARMA[2]

[1]M. F. Radar, Indian Institute of Geomagnetism,
Shivaji University Campus, Kolhapur - 416 004 (India)

[2]Space and Earth Science Laboratory, Department of Physics, Shivaji University, Kolhapur - 416 004 (India)

[3]Department of physics, D N College, Faizpur - 425 503 (India)

E-mail : rupesh_ghodpage@rediffmail.com

Abstract : Simultaneous photometric measurements of the OI 630.0 nm, OI 557.7 nm and OH band hydroxyl lines from a low latitude station, Kolhapur (16.8^0 N, 74.2^{0}E) for the period of Jan.Feb.2004 were analyzed to study the atmospheric waves (gravity and tidal) characteristics and associated processes on clear, moonless. We present the nocturnal intensity variations of the different airglow emission lines observed using multispectral photometer. The analysis of the recorded data shows the presence of both upward and downward propagating waves. Commonly observed wave periods are near values of the tidal periods with 6, 8 and 12 hours sub harmonics. The vertical wavelength of both short and long period waves lies between 22 to 132 Km.

Key Words : Tidal and gravity wave, Airglow, Harmonics and sub-harmonics

Introduction :

Atmospheric tides and gravity waves are the principal dynamic features of the mesospheric and lower thermospheric (MLT) regions and play an important role in transporting energy and momentum horizontally and vertically providing dynamical linkage between the lower atmosphere and the MLT region. Due to the solar radiative heating of water vapor in the troposphere and ozone in the stratosphere, atmospheric tides shows regular phases with harmonic periods of 24 hours and its sub harmonics (i.e. 12, 8, 6, 4 hrs etc). Tides are classified as migrating and non-migrating. Migrating tides are global scale waves following apparent motions of the Sun and propagates westward with dominant periods of 24 hrs and 12 hrs referred as diurnal and semi-diurnal tides respectively (1). The diurnal tides are mainly excited by direct absorption of sunlight by water vapor in the troposphere and stratosphere, whereas the semi-diurnal tides are mainly excited by ozone heating in the upper stratosphere and lower mesosphere. The wavy structures observed in the mesospheric nightglow intensity variations have also been attributed to the upward propagating gravity waves generated in the lower atmospheric regions (2-8). Taori (9) analyzed OH (6, 2) and O_2 (0, 1) airglow data collected and showed downward phase propagation. Using cross wavelet analysis, he showed the presence of strong quasi 8 hours wave at two altitudes (87 and 94 km) simultaneously.

In this paper, we present and discuss simultaneous observations of nightglow emissions of OH (7, 2) Meinel band, OI 557.7 nm and OI 630.0 nm at the low latitude station Kolhapur (16.8^{0}N, 74.2^{0}E) in India. The emission heights of OH (7, 2), OI 557.7 nm and OI 630.0 nm are 87, 97 and 250 km from the surface of the Earth respectively. The analysis yields characteristics features of vertical propagating tidal and gravity waves. Short and long period oscillations having periodicities 12, 8, and 6 hours have been observed.

Observations and analysis techniques :

Regular observations of the night airglow emissions, OH (7, 2), OI 557.7 nm and OI 630.0 nm have been carried out using multispectral photometer at Kolhapur on clear and moonless nights during the periods of January and

February 2004. The multispectral photometer unit takes about 2 minutes to complete one sequence of observations with five filters. The half field of view of the photometer is 7.25 deg. The filters employed have transmission efficiency ~ 60-70 % at 25^{0}C. In this study we have analyzed simultaneous observations of the OH (7, 2), OI 557.7 nm and OI 630.0 nm emissions, carried out during the period 2004. In the analysis method airglow intensity values of the OI 557.7 nm are averaged at an interval of 15 minutes. In this approach one can decipher wavy structures with periods more than 30 minutes (frequency ~ 1/2dT). Initially the variation of airglow intensity for each emission line for each night was plotted and scrutinized to check if there is any contamination in the data due to clouds or artificial lights.

(a) Harmonic analysis

In the present study, we have adopted a harmonic analysis technique to get the amplitudes and phases of different wave components or periods in the airglow data. In the technique, the variant X(t) can be represented by

$$\{X(t) = X \text{ (mean)} + \Sigma [Ai \sin\left(2\pi \frac{it}{T}\right) + Bi \cos\left(2\pi \frac{it}{T}\right)]\}$$

Where the coefficients A*i* and B*i* are given by

$$Ai = \frac{2}{N}\Sigma\left\{X \sin\left(2\pi \frac{it}{T}\right)\right\};\ Bi = \frac{2}{N}\Sigma\left\{X \cos\left(2\pi \frac{it}{T}\right)\right\};$$

Where, *i* can have any integer values between 1 to { QUOTE, $\left[\left(\frac{N}{2}\right) - 1\right]$ }, T is total data length, *t* is the time variation of the data. In the Fourier analysis technique, the first harmonic has a period equal to the total period of data length used. The second harmonic has a period equal to half the fundamental period, and so on. From equation (1) and (2) the amplitude and phase of the harmonics are given by

$$Xi = \sqrt{A^2 i + B^2 i} \text{ and } \emptyset i = \tan^{-1}\left(\frac{Ai}{Bi}\right) \quad \ldots (3)$$

(b) Tidal influence in airglow:

We have used the running averaged data at an interval of 15 minutes. In order to remove short period irregular trend in the data set, a code was developed in Mat Lab environment and applied to make the data set a stationery series (the first and the last values were made the same) and if jumps present in the data then it is removed. We have written code for curve fitting. There are different methods for fitting the curve getting the periodicities in a given data set. We have used a simple best fit cosine model (11) to get the different periods of waves. After fitting data with cosine model, we have evaluated the goodness of fit. For that we have also plotted airglow intensity residuals. The residuals approximate the random errors; therefore, if the residuals appear to behave randomly, it suggests that the model fits the data well. The cosine model is written as;

$$Y(t) = A_0 \cos\left[\frac{\pi(t-\emptyset)}{\tau}\right] \quad \ldots\ldots (4)$$

Where, A_0 is the amplitude of fitted curve of half period time T with phase Ö, and *t* is the time. From this equation we determine the time periods of different waves showing a semidiurnal nature in the cosine fit. The commonly observed features are waves near the tidal periods with 6, 8 and 12 hour oscillations.

Results and discussion :

In the present investigation, the nocturnal airglow intensity variations observed on several nights in OH (7, 2), OI 557.7 nm and OI 630.0 nm were used for computing the amplitude and phase of the different harmonics in the total data length of 9-10 hours per night, thereby inferring the directions of wave propagation in both upward and downward direction.

In fig. 1 the topmost panel shows the plot of OH (7, 2), OI 557.7 nm and OI 630.0 nm emission intensities recorded on February 14-15, 2004. It is clearly seen that the phase propagation is upward for the longer period waves (540 min) between the layers, OI 557.7nm and OI 630.0 nm and OH (7, 2) and OI 630 nm. Similar feature is also found in phase propagation between OH (7, 2) and OI 557.7 nm layers. Here we observed OI 557 nm wave leads 97.5 min than OH emission wave. In case of short period wave phase difference between OI557 nm and OH emission observed 37.5.Both OH and OI 557 nm, long period wave's phases are propagating in upward direction and also short

waves propagating in upward direction. Sometimes, the phases are in opposite direction and there is not much change in phases during the propagation.

If the separation of the layers and the phase differences are known one can compute the vertical wavelength (7). The ratio between the vertical wavelength and the horizontal wavelength uniquely defines the orientation and propagation direction of the wave. For waves with periods much larger than the Brunt Vaisala Period (say greater than 1 hour) and less than a few hours, relation describing the characteristics of internal gravity waves approximately applies (13). Also, knowing the vertical wavelength, horizontal wavelength of the wave can be computed (7). The vertical wavelength of short period wave (S) which varies between 37.6 km to 75.2 km and for long period wave (L) varies between the 33.2 km to 130.3 km propagation between OH (7, 2) and OI 557.7 nm emission layers.

The estimated phase velocities for the short period waves between OH (7, 2) and OI 557.7 nm layers vary between ~ 1.5 m/s to 21 m/s and time lag vary between ~ 7.5-120 min and long period phase velocity lies between ~ 1.08 m/s to ~ 45 m/s with time lag of ~ 15-180 min. In all the three emission lines OH (7, 2), OI 557.7 nm and OI 630.0 nm the long period wave phase velocity varies between ~ 2 to ~ 98 m/s and time lag vary between ~ 15-180 min.

Figure 2 shows the cosine fit curves, the panel (a) cosine fit of OI 557.7 nm and panel (b) cosine fit of OH (7, 2) emissions on the night of February 14-15, 2004. Solid line shows the best fit curve along with the 15 min running average airglow intensity data. It is seen that the period of OI 557.7 nm intensity variation is ~ 8 hours and OH (7, 2) emission period is ~ 12 hours. This matches well with the wave period of solar atmospheric tides (10). Thyaparan et al. (12) reported the significant contribution of 8 hours tide during spring and winter and less contribution during summer and fall time.

The fig. 3 portrays the airglow intensity residuals, which appear erratically, spread around zero showing the well fitted cosine model. Our results shows presence of short period waves propagating vertically upward. Vedas et al, (13) also reported similar features. The source of these wavy structures could be: (a) absorption of solar radiation by the atmospheric species present there, (b) the wave-wave or wave-tide interactions and development of instabilities which may grow and give rise to the observed wave features, interaction between different modes may give rise to other modes. Interaction between semi-diurnal and diurnal tides modes may result into the generation of 8 hours wave (14).

Conclusion :

Based on the observations and analysis the following conclusions are derived.

(1) Both upward and downward phase propagations are observed in long (540 min) and short (270 min) period waves. The long period wave may be due to the effect of atmospheric tides and short period waves may be due to gravity waves. Most (80%) of thelong period waves, the phase propagation is upward.

(2) The phase velocities of the short period waves propagating between OH (7,2) and OI 557.7 nm emissions are small between 1.52 m/s to 21 m/s, on the other hand upward velocities for long period waves are large 1.08 m/s to 45 m/s).

(3) We also observed semi-diurnal component of atmospheric tides often present in OH and OI 557.7 nm.

The result and analysis shows possibilities of propagation of gravity and tidal waves through mesosphere and thermosphere, even result in transporting energy. We plan to produce comprehensive database in order to further investigate this subject.

Acknowledgement :

The Department of Science and Technology (DST), Govt. of India, New Delhi funded the research in Upper Atmospheric Sciences in IIG. The night airglow observations at Kolhapur were carried out under the scientiûc collaboration pro-gram (MoU) between IIG, Panvel, and Shivaji University, Kolhapur.

Table - 1 : Phase velocity (m/s) calculated from distance between layers (ΔD) and phase difference ΔT (minutes) obtained from the harmonic analysis of the two emission lines OI 557.7 nm and OH.

Table. 1.					
S.N	Date	ΔT in (min)		V in (m/s)	
		(S)	(L)	(S)	(L)
1	17 Jan.2004	75	45	2.44	4.07
2	14 Feb.2004	37.5	97.5	4.44	1.88
3	15 Feb.2004	45	82	4.07	2.32
4	16 Feb.2004	45	75	4.07	2.44
5	17 Feb.2004	37.5	90	4.44	2.03
6	18 Feb.2004	7.5	15	20.44	45.22
7	19 Feb.2004	45	30	4.07	6.11
8	20 Feb.2004	120	180	1.52	1.08

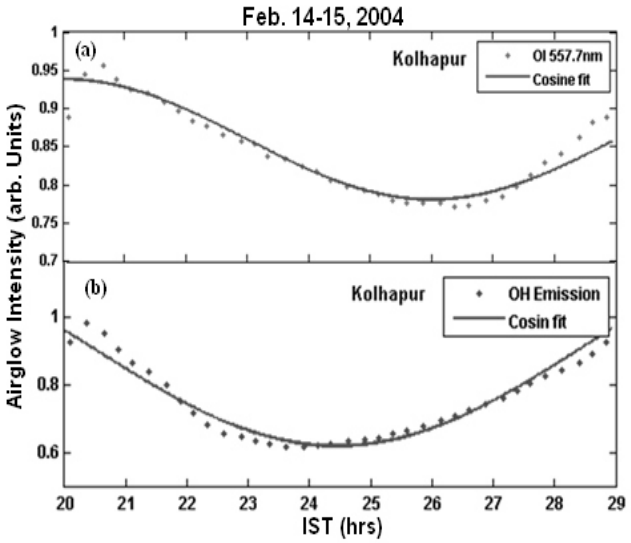

Fig. - 2 : The cosine fit of (a) OI 557.7 nm and (b) OH emission, on Feb, 14-15, 2004 at Kolhapur. The solid line curve shows best cosine fit analysis.

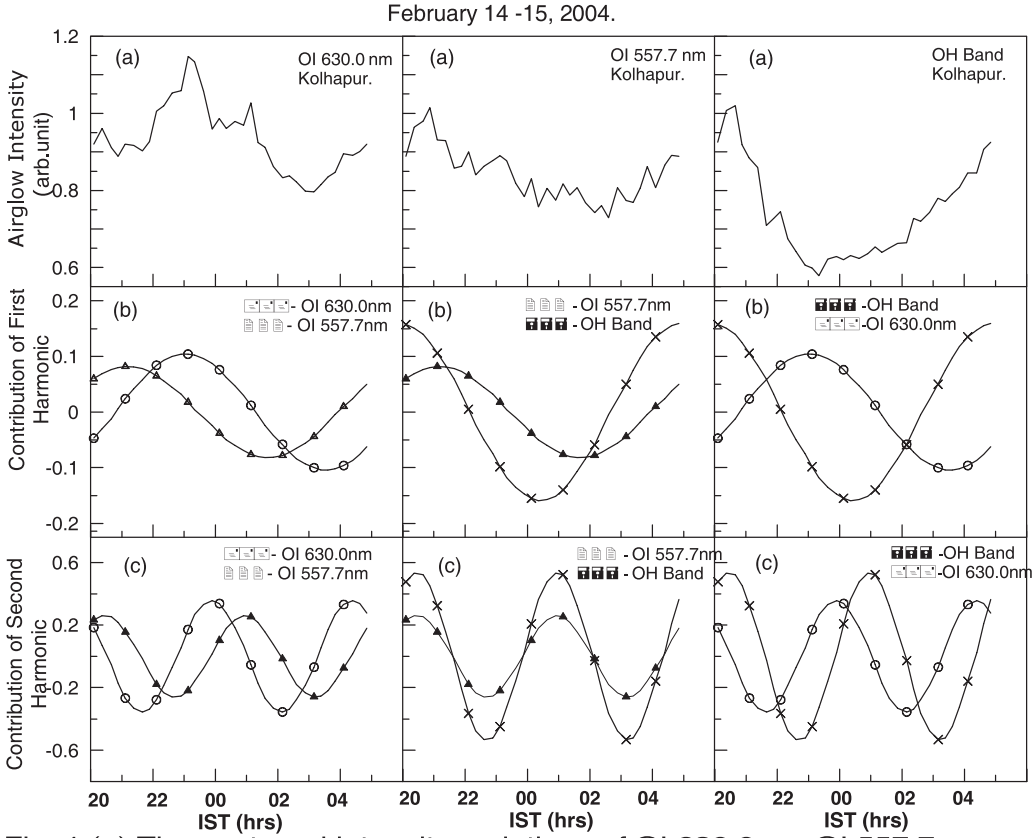

Fig. 1 (a) The nocturnal intensity variations of OI 630.0nm, OI 557.7nm and OH (7,2) emissions for the night of February 14-15, 2004 at Kolhapur, (b) Contribution of first harmonics, and (c) Contribution of second harmonics.

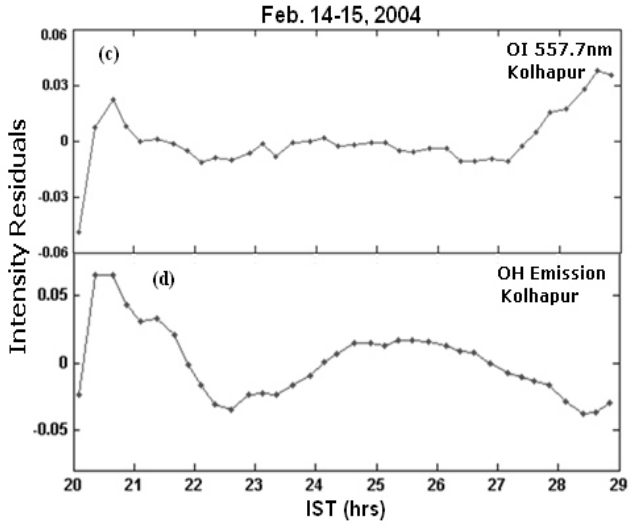

Fig. - 3 : The airglow intensity residuals (a) OI 557.7 nm and (b) OH emission, on Feb, 14-15, 2005 at Kolhapur.

References :

1] Chapman, S., Lindzen, R.S., Atmospheric Tides, D. Reidel Press, Dordrecht, Holland, 200 p **(1970).**

2] Krassovsky, V. I., Infrasonic variation of OH emission in the upper atmo-sphere, Ann. Geophys., **28,** 739–746 **(1972).**

3] Hines, C. O. and Tarasick, D. W., On the detection and utilization of gravity Waves in airglow studies, Planet.Space Sci., **35,** 851–866 **(1987).**

4] Tarasick, D.W., and Hines, C.O., The observable effects of gravity waves in airglow emissions, Planet. Space Sci., **38,** 1105-1119 **(1990).**

5] Tarasick, D. W., Shepherd, G. G., Effects of gravity waves on complex airglow chemistries. 1 O_2 ($b^1\Re^+g$) emission., J. Geophys. Res., **97,** 3185–3193 **(1992)a.**

6] Tarasick, D. W., Shepherd, G. G., Effects of gravity waves on complex airglow chemistries 2. OH emission. J. Geophys. Res., **97,** 3195–3208 **(1992)b.**

7] Fagundes, P. R., Takahashi H., Sahai Y., Gobbi D., Observations of gravity Waves from multi spectral mesospheric nightglow emissions observed at 23^0, S. J. Atmos. Terr. Phys., **57,** 395-405 **(1995).**

8] Nakamura, T., A. Higashikawa, T. Tsuda, and Matsushita, Y., Seasonal variations of gravity wave structures in OH airglow with a CCD imager at Shigaraki, Earth Planets Space, **51,** 897– 906 **(1999).**

9] Taori, A., Taylor, M., Dominant winter-time mesospheric wave signatures over a low latitude station, Hawaii (20.8^0 N N): An investigation, J. Earth System Sci., **119,** 259–264 **(2010).**

10] Shepherd, G.G., C. McLandress, and B.H. Solheim, Tidal influence on O(•S) airglow emission rate distributions at the geographic equator observed by WINDII, Geophys. Res. Lett., **22,** 275-278 **(1995).**

11] Taori, A., Guharay, A., Taylor, M. J., On the use of simultaneous measurements of OH and O2 emissions to investigate wave growth and dissipation, Ann. Geophys., **25,** 639–643 **(2003).**

12] Thayaparan, T. The terdiurnal tide in the mesosphere and lower thermosphere over London Canada (43^{0}N, 81^{0}W); Geophys. Res. Lett., **102,** 21695-21708 **(1997).**

13] Vadas, S. L., Fritts, D. C., Thermospheric response to gravity wave: Influence of increasing viscosity and thermal diffusivity. J. Geophys. Res., 110, D15103, doi: 10.1029/2004JD005574 **(2004).**

14] Taylor, M. J., Pendleton, Jr. W. R., Gardner, C. S. and States, R. J. Comparison of terdiurnal tidal oscillations in mesospheric OH rotational temperature and Na lidar temperature measurements at mid-latitudes for fall/spring conditions; Earth Planets Space, **51,** 877-885 **(1999).**